Two-dimensional Kagome Lattices Made of Hetero Triangulenes are Dirac Semimetals or Single-Band Semiconductors

Yu Jing[1,2], Thomas Heine[1,2,3,*]

1 Wilhelm-Ostwald-Institut für Physikalische und Theoretische Chemie, Linnéstr. 2, 04103 Leipzig, Germany;

2 TU Dresden, Fakultät Chemie und Lebensmittelchemie, Bergstraße 66c, 01062 Dresden, Germany.

3 Helmholtz-Zentrum Dresden-Rossendorf, Forschungsstelle Leipzig, Permoserstraße 15, 04318 Leipzig, Germany

Keywords: 2D COFs, single band semiconductors, Dirac semimetals, Kagome lattices, density functional theory

Abstract

In two dimensions, 11 lattice types are mathematically possible, the Kepler nets, but nature offers only few of them in dense crystals. Two-dimensional covalent organic frameworks (2D COFs) offer to overcome this limitation and to provide nets that are to date only possible as photonic lattices or atom-by-atom engineered surface structures. Here we discuss, based on first-principles calculations, 2D kagome lattices composed of polymerized hetero-triangulene units, planar molecules with D_{3h} point group containing a B, C or N center atom and CH_2, O or CO bridges. We explore the design principles for a functional lattice made of COFs, which involves control of π-conjugation and electronic structure of the knots. The former is achieved by the chemical potential of the bridge groups, while the latter is controlled by the heteroatom. The resulting 2D kagome COFs have a characteristic electronic structure with a Dirac band sandwiched by two flat bands and are either Dirac semimetals (C center), or single-band semiconductors - materials with either exclusively electrons (B center) or holes (N center) as charge carriers of very high mobility, reaching values of up to ~8×10^3 $cm_2V^{-1}s^{-1}$, which is comparable to crystalline silicon. The flat bands show a delocalized electronic structure with no contribution from the center atoms,

and their curvature is modulated by the bridge atoms. This suggests that the flat bands are inherent features of the kagome lattice.

Table of Contents graphic

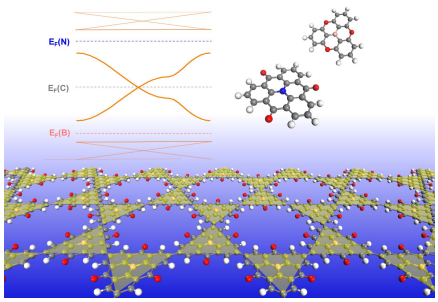

Introduction

The properties of a crystalline material are governed by both its lattice geometry and chemical composition. A simple and typical example highlighting the importance of the lattice is the two-dimensional (2D) honeycomb structure of graphene[1], where the characteristic Dirac cones emerge due to the two hexagonal sub-lattices. Already in 1619 Johannes Kepler reported that only 13 nets with identical knots are possible in two dimensions (as 2 of are enantiomeric today we talk about 11 Kepler nets).[2,3] Various derivatives of these Kepler nets are possible, an overview can be found, for example, in ref. 4. However, even fewer than the 11 Kepler nets are found in single-layers exfoliated from natural layered crystals, or on surfaces. As the importance of topology is evident, e.g. from the graphene example, it is intriguing to explore and potentially to exploit the properties of the remaining Kepler nets and of their derivatives.

laser writing technique it was possible to produce, e.g., the Lieb lattice, a superstructured square lattice.[21,22] In 2017, the electronic Lieb lattice was created by single-atom manipulation at a metal surface.[23-25] While both experiments confirm the intriguing predicted properties of the Lieb lattice, experimental realization requires challenging conditions, most importantly ultracold environment, which is a showstopper for real-world applications.

Molecular framework materials, such as metal-organic frameworks (MOFs)[26] and covalent-organic frameworks (COFs)[27] offer new possibilities to form exotic nets, because molecules, acting as knots, can be designed in such way that their bridging sites reflect the required topology of the net. 2D COFs (also called 2D polymers) offer the opportunity to create exotic lattices, such as square,[28] rectangular,[29] honeycomb,[27,30] Kagome (**kgm**)[31-33] and potentially Lieb lattice structures, which are stable at ambient conditions. 2D COFs have been fabricated by using surface-[34,35] or interface-[36,37] polymerization, and mechanical exfoliation of the layered bulk sometimes is possible.[38,39] However, in order to realize the desired topological properties of the exotic nets present in the 2D COFs, the molecules marking the knots

need to interact electronically with each other. In most cases, the bonds created by the coupling reaction electronically separate the π systems of the monomer units and thus block ballistic charge transport. Full sp^2 conjugation can be achieved if a C=C bond connects the extended monomers to form 2D COFs.[40,41] Also for the recently reported 2D COFs realized by surface calcination or solution synthesis of hetero-triangulenes (HTs),[42-44] which form the exotic **kgm** 2D net, intermolecular π conjugation is expected due to the disperse features in their band structure.

HTs are nearly planar molecules (the selection that is subject of this work is displayed in Figure 1a-f) that have been experimentally studied intensively.[45-49] We note here that in the reported band structures (Refs. 43 and 50) Dirac cones can be anticipated (we confirm them here), even though the HT centre atoms, which mark the knots of the honeycomb lattice, are separated by distances of more than 1 nm.

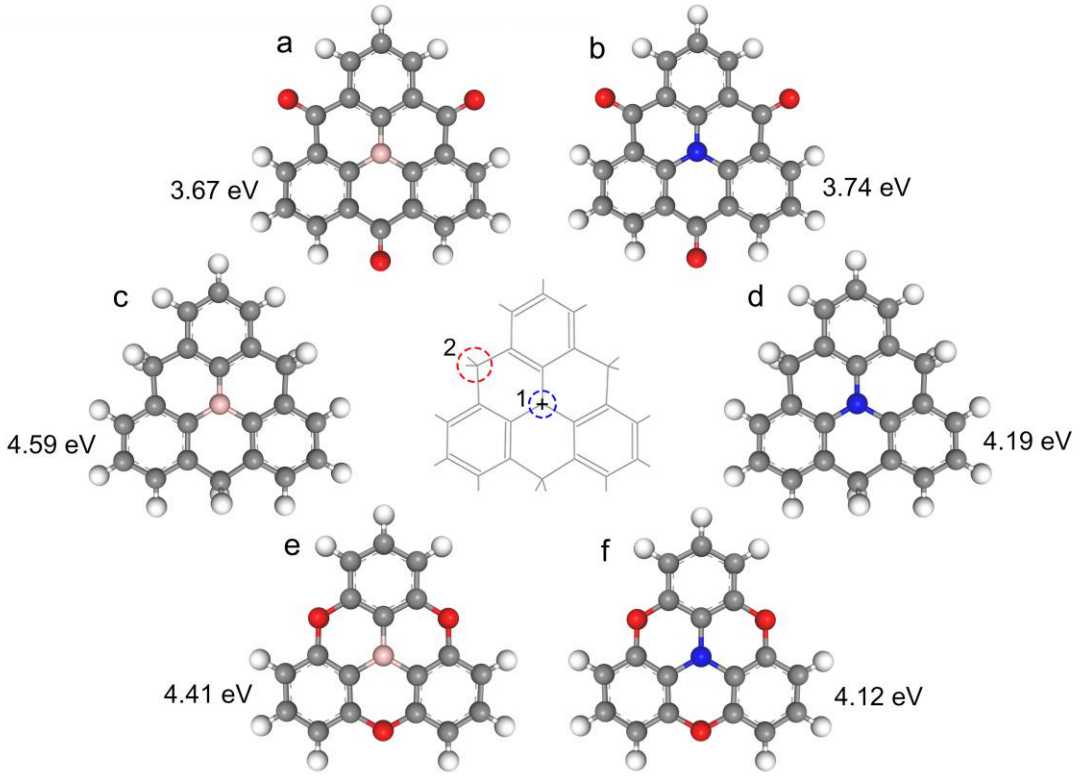

Figure 1. Schematic representation of cationic triangulene (centre) and its HTs derivatives by replacing the centred C^+ (1) with B or N, and the -CH_2 bridge (2) with C=O, or O, respectively, which are (a) carbonyl-bridged triphenylborane (CTPB), (b) carbonyl-bridged triphenylamine (CTPA),[45] (c) methylene-bridged triphenylborane (MTPB), (d) methylene-bridged triphenylamine (MTPA),[43] (e) oxygen-bridged triphenylborane (OTPB),[48] and (f) oxygen-bridged triphenylamine (OTPA);[49] the grey, white, red, blue and pink balls denote C, H, O, N and B, respectively.

Here, we show that 2D HT-based **kgm** lattices inhibit unprecedented electronic

features that are accessible by chemical modification of the building units. The intermolecular electronic overlap between the electronic π systems of the HT monomers in the **kgm** lattice can be tuned by the C=O, CH_2 or O bridges (see Figure 1). The HTs act as "superatoms" with local D_{3h} symmetry, in analogy to sp^2 hybridized C atoms. If the center atom is chosen to be carbon (HT(C)), the monomers also electronically act like sp^2 hybridized carbon atoms, and arranging six of them in a "superbenzene" structure, a D_{3h} $(HT)_6$-oligomer as shown in Figure 2a, results in frontier π orbitals that resemble the characteristic electronic structure of benzene, which is prototypic for aromatic molecules. Arranged in an extended 2D **kgm** lattice (Figure 2b), the electronic structure includes the expected half-filled Dirac cones at the K points of the Brillouin zone (Figure 2c). If the heteroatoms are changed to B or N, the resulting **kgm** lattices show a peculiar combination of two apparently mutually exclusive characteristics (Figure 2c): one of the bands next to the Fermi level is flat and does not contribute to charge transport, the other one is strongly dispersed, with highly mobile charge carriers (reaching mobility of 8×10^3 $cm^2V^{-1}s^{-1}$ in the case of **kgm** CTPB-COF), and thus determines the electric conductivity. The **kgm** HT-COFs become either n-type (only electrons as mobile charge carriers) or p-type (only holes as mobile charge carriers) single band (intrinsic) semiconductors, by either completely emptying (B) or filling (N) the strongly dispersed Dirac bands (Figure 2c).

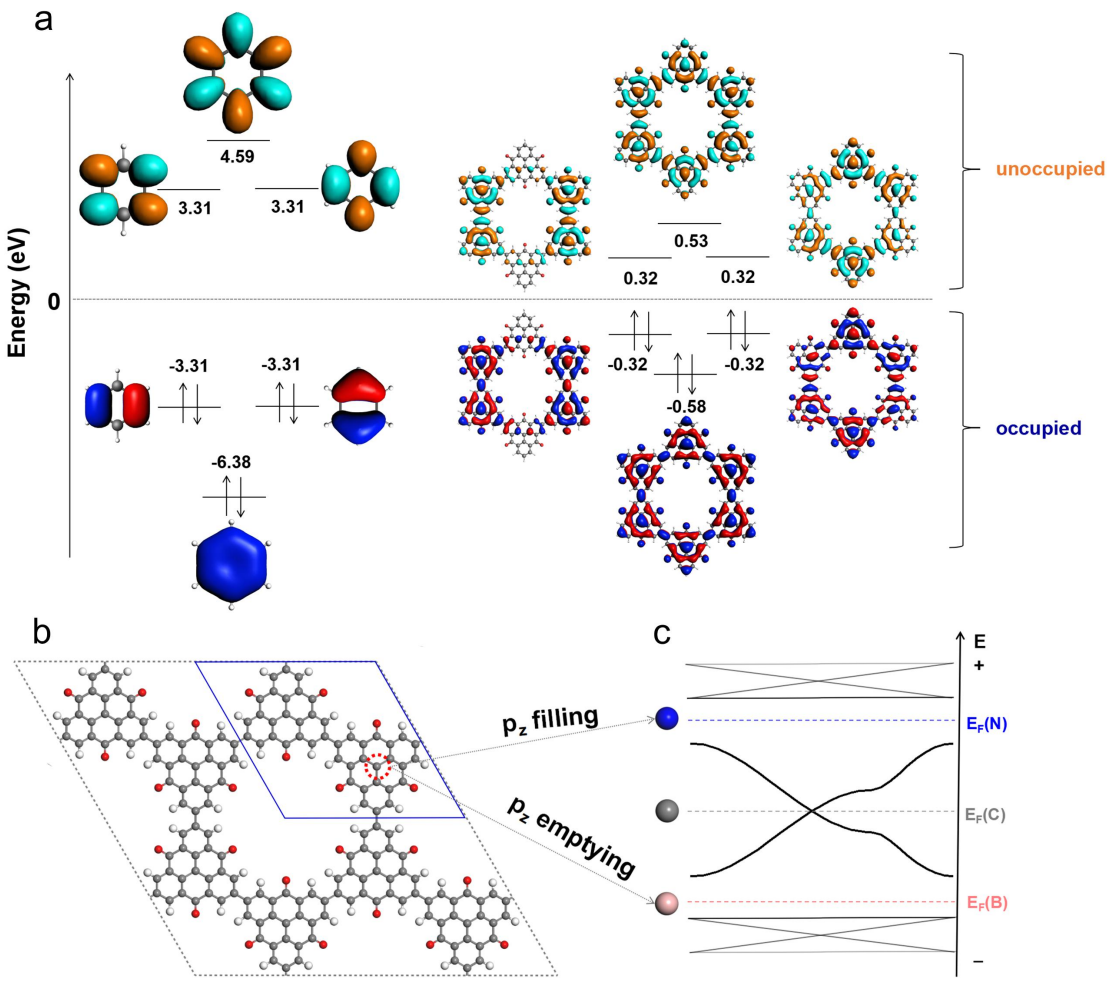

Figure 2. (a) Frontier molecular orbitals and schematics of energy levels for D_{3h} carbonyl-bridged triphenylmethyl radical (CTP) oligomer (D_{3h} $(CTP)_6$) in comparison with those of benzene. Akin to benzene ring, the frontier orbitals of D_{3h} $(CTP)_6$ are degenerate (the HOMO/HOMO-1 orbitals, and LUMO/LUMO+1 orbitals), and show significant π-conjugation. Similar results are found for the methylene-bridged triphenylmethyl radical (MTP) and oxygen-bridged triphenylmethyl radical (OTP) based oligomers. The dashed line represents the isolated p orbitals and is set to be 0 eV. (b) a **kgm** CTP-COF structure in a 2×2×1 supercell, the unit cell is indicated by the blue line; (c) centre-atom dependent band structure. Neutral C centered **kgm** HT-COFs show Dirac bands, which get filled or emptied by N or B substitution, respectively, resulting in semiconductors with mobile p- or n-type charge carriers. EF(N), EF(C) and EF(B) denote the positions of the Fermi levels of corresponding **kgm** HT(N/C/B)-COFs. The grey, white, red, blue and pink balls denote C, H, O, N and B, respectively.

Results and Discussion

kgm *COF structures assembled from HT monomers*

Highly reactive triangulene is a π radical with two unpaired electrons.[51] Stable cationic closed-shell derivatives are obtained by substitution of outer CH groups with CO, O, or CH_2 bridges (Figure 1). Such molecular ions have been widely used as dyes.[52] As neutral, single radical species, their D_{3h} symmetry allows the arrangement in a honeycomb, precisely in a **kgm** lattice (which combines a regular hexagonal tiling and a regular triangular tiling), thus forming a **kgm** 2D COF. The frontier orbital of the HT(C)s has π character with one unpaired electron and resembles the electronic features of sp^2 carbons in aromatic molecules, illustrated for a benzene-analogue of CTP in Figure 2a. If arranged in a honeycomb lattice, a band resembling the graphene frontier bands is formed, i.e. with Dirac cones at the K points of the Brillouin zone (Figure 3 b, e, h). In free-standing form, for steric reasons, the monomers are slightly twisted with respect to one another, which results in the opening of a small band gap of 29~58 meV (Figure S1). Note that the honeycomb lattice points in the **kgm** HT(C)-COFs have a next-neighbor distance of 0.99~1.01 nm, seven times larger than in graphene.

On the other hand, the substituted HTs resemble the electronic analogues of 2D nitrogen (N-substituted) and 2D boron (B-substituted), both in honeycomb structure. While B and N substituted graphene has been discussed in the literature,[53] the electronic analogues to the HT(C)-COFs would be 2D honeycomb all-boron or all-nitrogen lattices, respectively, both being instable and not known in nature. The six substituted HT(N/B)s structures are shown in Figure 1a-f, all of these molecules being nearly planar and with HOMO-LUMO gaps in the range of 3.7-4.6 eV. The resulting **kgm** HT(N/B)-COFs are stable (two have been reported experimentally),[42,43] and for all others the reaction energy is very similar, ranging from 1.36...1.86 eV/unit (see Equation S1, Table S1 and Figure S2). They all have similar lattice vectors (17.07…17.62 Å) and pore sizes (11.75…13.10 Å) (Table S1), where the HT(B)-COFs always show somewhat larger lattice constants and pore sizes than their

N centered counterparts. In free-standing form, the **kgm** HT(N/B)-COFs are slightly twisted. In the remainder, however, we assume them to adopt flat geometries in agreement with a suspended structure as expected in experiment (see refs. 42,43). However, even if they are slightly twisted, their electronic characteristics are maintained and the twisting has negligible impact on the results presented and discussed here (for details, see Figure S3 and Table S1 and 2).

*Electronic properties of the **kgm** HT-COFs*

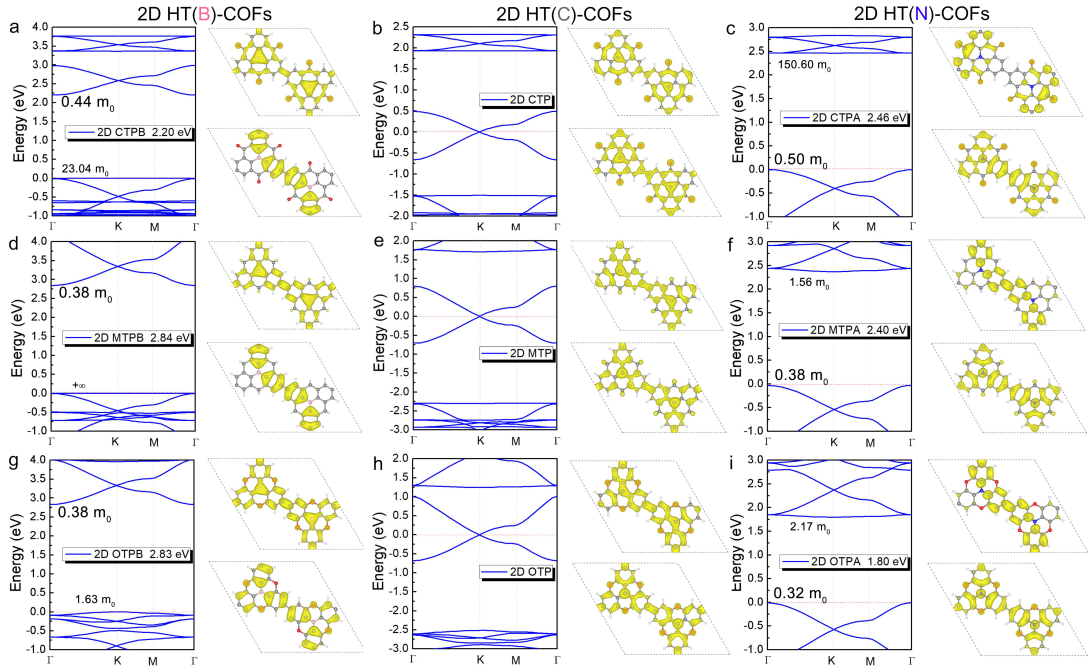

Figure 3. (a-i) band structures and charge density distribution for the frontier bands (above for CBM and below for VBM, respectively) of **kgm** HT(B/C/N)-COFs as introduced in Figure 1a-f. 2D MTP and OTP complete the **kgm** HT(C)-COFs built from MTP radical and OTP radical. The calculations were performed using the HSE06 functional, the Fermi level is set at the VBM for the semiconductors, effective masses of the frontier bands are indicated, and the isosurface for all orbitals is set to be 0.0013 eÅ^{-3}.

According to their band structures, the triangulene-based **kgm** COFs can be categorized in three classes (see Figure 3): **kgm** HT(C)-COFs are Dirac semimetals, and the **kgm** HT(N/B)-COFs are intrinsic single-band semiconductors with electrons (HT(B)-COFs) and holes (HT(N)-COFs) as mobile charge carriers. Band structures, band gaps, effective masses and frontier crystal orbitals are given in Figure 3. The band gaps range from 1.8-2.8 eV, with the band edges being enclosed within the

HOMO-LUMO region of their corresponding HT(N/B) monomers (Figure S4). In all cases, the flat bands have their extrema (if they can be specified) at the K point, while those of the strongly dispersed band is located at the Γ point. Even though the effective masses of the mobile charge carriers are similar, ranging from 0.32-0.5 m_0 (Figure 3, Table S3), the calculated charge carrier mobilities (see Equation S2, Table 1, Figure S5) differ strongly between the **kgm** HT(N)-COFs (0.5-0.9 $\times 10^3$ $cm^2V^{-1}s^{-1}$) and their generally more mobile **kgm** HT(B)-COF counterparts (0.8-8.4 $\times 10^3$ $cm^2V^{-1}s^{-1}$). For the flat bands, the lowest effective masses are 1.6 m_0, while for some structures the effective masses exceed 100 m_0.

Table 1. Calculated effective masses m* for electrons and holes (values for low-mobility carriers are given in italic). For the mobile charge carriers, deformation potential (DP) constant E_1, in-plane stiffness C_{2D} and carrier mobility μ for **kgm** HT(N/B)-COFs along the zigzag direction. Armchair values differ only slightly (see Table S4). The calculations were performed at the PBE level of theory.

kgm HT-COFs	CTPB	CTPA	MTPB	MTPA	OTPB	OTPA
m_e^*/m_0	0.44	*150.60*	0.34	*1.56*	0.35	*2.17*
m_h^*/m_0	*23.04*	0.47	∞	0.30	*1.63*	0.27
E_1 /eV	0.72	2.21	2.09	3.87	2.97	4.78
C_{2D} /Nm^{-1}	59.32	63.25	59.79	62.73	65.05	63.72
μ /× 10^3 $cm^2V^{-1}s^{-1}$	8.4	0.8	1.7	0.7	0.9	0.5

The triangulene derivatives behave as “superatoms” B, C and N, where an sp^2–like configuration is enforced by the D_{3h} symmetry and planarity of the molecules, and a π-orbital resembling the $2p_z$, which is either empty (B), half-filled (C) or filled (N). Orbitals of the flat bands (Figure S6) show no contribution of the HT center atoms (independent of C, N or B), but are delocalized on the remainder of the 2D lattice. Functionalization of the bridge controls the π conjugation and thus the HOMO-LUMO gap of the HT molecules (it decreases from CH_2 via O to CO bridges both for B- and N-HTs), and consequently the band gap of the **kgm** HT(N/B)-COFs, which is smaller due to π conjugation and dispersion of the frontier band. Bridge functionalization controls the orbital shapes of the HT(N/B) molecules and thus the

conjugation in the **kgm** HT(N/B)-COFs, in particular the curvature of the flat bands. In the case of very flat bands (VB of **kgm** CTPB-COF and MTPB-COF, CB of **kgm** CTPA-COF) the π electron density is significant at the bridge groups, but vanishes at the bonds connecting the monomers (Figure 3). On the other hand, appreciable conjugation is observed for the more dispersed flat bands (VB of **kgm** OTPB-COF, CB of **kgm** MTPA-COF and OTPA-COF). Partial density-of-states (PDOS) analysis (Figure S7) indicates that the C=O bridge has significant contribution at the VBM of **kgm** CTPB-COF and CBM of CTPA-COF, contrary to CH_2 and O bridges. The conjugated band with the low-effective-mass charge carriers is less affected, but this picture changes for charge carrier mobilities, where both center atom and bridge group strongly affect the electron-phonon coupling via the deformation potential (DP, See Equation S2): the holes in **kgm** HT(N)-COFs are more prone to acoustic phonon scattering than the electrons of **kgm** HT(B)-COFs that possess the same bridge skeleton, while the C=O, CH_2 and O bridges reduce the carrier mobilities in that order, but with smaller impact. Note that due to neglect of coupling between optical phonons and electrons our predicted charge carrier mobilities are likely to be slightly overestimated.

Conclusion

To summarize, we have shown that hetero-triangulene derivatives act like sp^2 "superatoms" B, C or N. In a honeycomb structure, the lattice points are more ~1 nm apart from each other, still considerable interaction is present as reflected in the highly dispersed π band that governs the electronic properties of the presented 2D COFs. The six **kgm** HT(B/N)-COFs are intrinsic semiconductors with band gaps in the range of 1.8-2.8 eV, so their charge carriers must be activated, for example by chemical or gate doping, or by photoexcitation. The center atom (B or N) determines the type of mobile charge carrier, while the bridge functional group influences band gap and degree of π conjugation. While one frontier band shows very high charge carrier mobility of up to 8×10^3 $cm^2V^{-1}s^{-1}$, the other bands do not contribute to charge transport. Those flat bands contribute high peaks in the electronic density-of-states

and may offer interesting phenomena, as for example Lifshitz transitions[54] if located at the Fermi level. Our observations suggest that the flat bands are inherent features of the **kgm** lattice, as their crystal orbitals are formed by all atoms except for the center ones, and as their dispersion is strongly influenced by the bridge groups which mark the edges of the triangles that characterize the **kgm** lattice structure.

We believe that 2D COFs offer the possibility to realize all 11 Kepler nets, and also its derivatives such as the Lieb lattice. The prerequisites are flat monomers with extended π conjugation and connection points specific to the desired net, and conjugation-preserving coupling reactions. Moreover, the large distance between the knots (here: 1 nm) may allow post-synthetic modification with surface modification techniques. To fully explore this emerging field of chemistry, it is important to develop alternative coupling reactions that go from on-surface calcination to solution synthesis.

Methods

The structures of HT(N/B)s were optimized by using Amsterdam Density Functional (ADF) package.[55]

The lattices of **kgm** COFs were optimized by employing first-principles calculations on basis of density functional theory (DFT), as implemented in Vienna *ab initio* simulation package (VASP).[56] An efficient memory conserving symmetrization of the charge density is used. Projector-augmented plane wave (PAW) approach was employed to describe the ion−electron interactions.[57] All calculations have first been carried out using the PBE functional,[58] and electronic structures have been refined by the Herd−Scuseria−Ernzerhof hybrid functional (HSE06).[59] All the examined 2D **kgm** structures have a diamagnetic ground state. For more details on method validation, structural stability, electronic calculations, please see SI.

Supporting Information

The Supporting Information is available free of charge on the ACS Publications Website at DOI:xxxxxxxx.

Details of the DFT calculation, frontier orbitals of HTs oligomers, stability of **kgm**

HT(N/B)-COFs, band structure of twisted **kgm** HT-COFs and details for the calculations of the carrier mobilities according to the DP theory, orbitals of the flat bands and density of states of **kgm** HT(N/B)-COFs are given in the Supporting information.

Corresponding Author

*E-mail: thomas.heine@tu-dresden.de

Author Contributions

The manuscript was written through contributions of all authors. All authors have given approval to the final version of the manuscript.

Notes

The authors declare no competing financial interest.

Acknowledgement

The authors are grateful to the financial support by FlagERA (DFG HE 3543/27-1) and by the H2020 Marie Skłodowska–Curie Actions (H2020-MSCA-IF-2016, No.751848). We thank ZIH Dresden for a computer time grant.

References

(1) Novoselov, K. S.; Geim1, A. K.; Morozov, S. V.; Jiang, D.; Katsnelson, M. I.; Grigorieva, I. V.; Dubonos, S. V.; Firsov, A. A. *Nature* **2005**, *438*, 197–200.

(2) Kepler, J. Weltharmonik II. Buch der Weltharmonik. München – Berlin: R. Oldenbourg Verlag, **1939**, P. 63; Original: Harmonice Mundi, 1619.

(3) Coxeter, H. S. M. Regular polytopes, Dover Publications: Third Edition, New York, **1973**, P. 14, 69, 149.

(4) Smirnova, N. L. On Kepler-Shubnikov nets. *Crystallogr. Rep*. **2009**, *54*, 743.

(5) Delplace, P.; Ullmo, D.; Montambaux, G. *Phys. Rev. B* **2011**, *84*, 195452.

(6) Liu, Z.; Wang, Z. F.; Mei, J. W.; Wu, Y. S.; Liu, F. *Phys. Rev. Lett*. **2013**, *110*, 106804.

(7) Liu, F.; Wakabayashi, K. *Phys. Rev. Lett*. **2017**, *118*, 076803.

(8) Gouveia, J. D.; Maceira, I. A.; Dias, R. G. *Phys. Rev. B* **2016**, *94*, 195132.

(9) Terrones, H.; Terrones, M.; Hernandez, E.; Grobert, N.; Charlier, J. C.; Ajayan, P. M. *Phys. Rev. Lett*. **2000**, *84*, 1716.

(10) Lisenkov, S. V.; Vinogradov, G. A.; Astakhova, T. Y.; Lebedev, N. G. *JETP Letters*, **2005**, *81*, 346–350.

(11) Weeks, C.; Franz, M. *Phys. Rev. B* **2010**, *82*, 085310.

(12) Karenin, A. A. *J. Phys. Conf. Ser*. **2012**, *345*, 012025.

(13) Gouveia, J. D.; Dias, R. G. *J. Magn. Magn. Mater*. **2015**, *382*, 312–317.

(14) Dias, R. G.; Gouveia, J. D. *Sci. Rep.* **2015**, *5*, 16852.

(15) Goldman, N.; Urban, D. F.; Bercioux, D. *Phys. Rev. A* **2011**, *83*, 063601.

(16) Van Miert, G; Smith, C. M. *Phys. Rev. B* **2016**, *93*, 035401.

(17) Gouveia, J. D.; Dias, R. G. *J. Magn. Magn. Mater*. **2016**, *405*, 292–303.

(18) Sarkar, S.; Langer, S; Schachenmayer, J.; Daley, A. J. *Phys. Rev. A* **2014**, *90*, 023618.

(19) Schachenmayer, J.; Weld, D. M.; Miyake, H.; Siviloglou, G. A.; Ketterle, W.; Daley, A. J. *Phys. Rev. A* **2015**, *92*, 041602.

(20) Kantian, A.; Langer, S.; Daley, A. J. *Phys. Rev. Lett*. **2018**, *120*, 060401.

(21) Vicencio, R.; Cantillano, C.; Morales-Inostroza, L.; Real, B.; Mejía-Cortés, C.; Weimann, S.; Szameit, A.; Molina, M. I. *Phys. Rev. Lett.* **2015**, *114*, 245503.

(22) Mukherjee, S.; Spracklen, A.; Choudhury, D.; Goldman, N.; Öhberg, P.; Andersson, E.; Thomson, R. R. *Phys. Rev. Lett.* **2015**, *114*, 245504.

(23) Slot, M. R.; Gardenier, T. S.; Jacobse, P. H.; van Miert, G. C.; Kempkes, S. N.; Zevenhuizen, S. J.; Smith, C. M.; Vanmaekelbergh, D.; Swart, I. *Nat. Phy.* **2017**, *13*, 672.

(24) Drost, R.; Ojanen, T.; Harju, A.; Liljeroth, P. *Nat. Phys.* **2017**, *13*, 668.

(25) Bercioux, D.; Otte S. *Nat. Phys.* **2017**, *13*, 628–629.

(26) Li, H.; Eddaoudi, M.; O'Keeffe, M.; Yaghi, O. M. *Nature* **1999**, *402*, 276.

(27) Côté, A. P.; Benin, A. I.; Ockwig, N.W.; O'Keeffe, M.; Matzger, A. J.; Yaghi, O. M. *Science* **2005**, *18*, 1166–1170.

(28) Kandambeth, S.; Shinde, D. B.; Panda, M. K.; Lukose, B.; Heine, T.; Banerjee, R. *Angew. Chem.* **2013**, *125*, 13290–13294.

(29) Huang, N.; Zhai, L.; Coupry, D. E.; Addicoat, M. A.; Okushita, K.; Nishimura, K.; Heine, T.; Jiang, D. *Nat. Comm*. **2016**, *7*, 12325.

(30) Kandambeth, S.; Mallick, A.; Lukose, B.; Mane, M. V.; Heine, T.; Banerjee, R. *J. Am. Chem. Soc*. **2012**, *134*, 19524-19527.

(31) Huang, N.; Wang, P.; Jiang, D. *Nat. Rev. Mater*. **2016**, *1*, 16068.

(32) Feng, X.; Ding, X.; Jiang, D. *Chem. Soc. Rev.* **2012**, *4*1, 6010–6022.

(33) Waller, P. J.; Gándara, F; Yaghi, O. M. *Acc. Chem. Res*. **2015**, *48*, 3053–3063.

(34) Xu, L.; Zhou, X.; Tian, W. Q.; Gao, T.; Zhang, Y. F.; Lei, S.; Liu, Z. F. *Angew. Chem. Int. Ed*. **2014**, *53*, 9564–9568.

(35) Liu, X. H.; Guan, C. Z.; Ding, S. Y.; Wang, W.; Yan, H.-J.; Wang, D.; Wan, L. J. *J. Am. Chem. Soc*. **2013**, *135*, 10470–10474.

(36) Dai, W.; Shao, F.; Szczerbiński, J.; McCaffrey, R.; Zenobi, R.; Jin, Y.; Schlüter, A. D.; Zhang, W. *Angew. Chem. Int. Ed*. **2016**, *55*, 213–217.

(37) Müller, V.; Shao, F.; Baljozovic, M.; Moradi, M.; Zhang, Y.; Jung, T.; Thompson, W. B.; King, B. T.; Zenobi, R.; Schlüter, A. D. *Angew. Chem. Int. Ed*. **2017**, *129*, 15464–15468.

(38) Biswal, B. P.; Chandra, S.; Kandambeth, S.; Lukose, B.; Heine, T.; Banerjee, R. *J. Am. Chem. Soc*. **2013**, *135*, 5328–5331.

(39) Chandra, S.; Kandambeth, S.; Biswal, B. P.; Lukose, B.; Kunjir, S. M.; Chaudhary, M.; Babarao, R.; Heine, T.; Banerjee, R.l *J. Am. Chem. Soc*. **2013**, *135*, 17853–17861.

(40) Jin, E.; Asada, M.; Xu, Q.; Dalapati, S.; Addicoat, M. A.; Brady, M. A.; Xu, H.; Nakamura, T.; Heine, T.; Chen, Q.; Jiang, D. *Science* **2017**, *357*, 673–-676.

(41) Zhuang, X.; Zhao, W.; Zhang, F.; Cao, Y.; Liu, F.; Bi, S.; Feng, X. *Polym. Chem*. **2016**, *7*, 4176–4181.

(42) Bieri, M.; Blankenburg, S.; Kivala, M.; Pignedoli, C. A.; Ruffieux, P.; Müllen, K.; Fasel, R. *Chem. Commun*. **2011**, *47*, 10239–10241.

(43) Steiner, C.; Gebhardt, J.; Ammon, M.; Yang, Z.; Heidenreich, A.; Hammer, N.; Görling, A.; Kivala, M.; Maier, S. *Nature Comm*. **2017**, *8*, 14765.

(44) Schlütter, F.; Rossel, F.; Kivala, M.; Enkelmann, V.; Gisselbrecht, J.-P.; Ruffieux, P.; Fasel, R.; Müllen, K. *J. Am. Chem. Soc*. **2013**, *135*, 4550–4557.

(45) Field, J. E.; Venkataraman, D. *Chem. Mater*. **2002**, *14*, 962–964.

(46) Zhou, Z.; Wakamiya, A.; Kushida, T.; Yamaguchi, S. *J. Am. Chem. Soc*. **2012**, *134*, 4529–4532.

(47) Hellwinkel, D.; Melan, M. *Chem. Ber*. **1974**, *107*, 616.

(48) Kitamoto, Y.; Suzuki, T.; Miyata, Y.; Kita, H.; Funaki, K.; Shuichi, O. *Chem. Commun*. **2016**, *52*, 7098–7101.

(49) Kuratsu, M.; Kozaki, M.; Okada, K. *Angew. Chem. Int. Ed*. **2005**, *44*, 4056–4058.

(50) Gutzler, *R. Phys. Chem. Chem. Phys.* **2016**, *18*, 29092–29100.

(51) Pavliček, N.; Mistry, A.; Majzik, Z.; Moll, N.; Meyer, G.; Fox, D. J.; Gross, L. *Nature Nanotech.* **2017**, *12*, 308–311.

(52) Bosson, J.; Gouin, J.; Lacour, J. *Chem. Soc. Rev.* **2014**, *43*, 2824–2840.

(53) Rania, P.; Jindal, V. K. *RSC Adv.* **2013**, *3*, 802–812.

(54) Lifshitz, I. M. *J. Exptl. Theoret. Phys. (U.S.S.R.)* **1960**, *38*, 1569–1576.

(55) te Velde, G.; Bickelhaupt, F. M.; Baerends, E. J.; Fonseca Guerra, C.; van Gisbergen, S. J. A.; Snijders, J. G.; Ziegler, T. *J. Comput. Chem*. **2001**, *22*, 931–967.

(56) Kresse, G.; Hafner, J. *Phys. Rev. B: Condens. Matter Mater. Phys*. **1993**, *47*, 558–561.

(57) Blöchl, P. E. Phys. Rev. B: Condens. *Matter Mater. Phys*. **1994**, *50*, 17953–17979.

(58) Perdew, J. P.; Burke, K.; Ernzerhof, M. *Phys. Rev. Lett*. **1996**, *77*, 3865–3868.

(59) Heyd, J.; Peralta, J. E.; Scuseria, G. E.; Martin, R. L. *J. Chem. Phys*. **2005**, *123*, 174101.